

Published in IET Science, Measurement and Technology  
Received on 9th July 2007  
Revised on 2nd November 2007  
doi: 10.1049/iet-smt:20070055



# Electromagnetic compatibility analysis of unstructured mains networks for high-speed data transmission: Part 1

S. Battermann<sup>1</sup> H. Garbe<sup>1</sup> F. Silva<sup>2</sup> M. Pous<sup>2</sup>  
V. Beauvois<sup>3</sup> K. Vantomme<sup>4</sup> J. Catrysse<sup>4</sup> J. Newbury<sup>5</sup>  
V. Degardin<sup>6</sup> M. Liénard<sup>6</sup> P. Degauque<sup>6</sup> I.D. Flintoft<sup>7</sup>  
A.D. Papatsoris<sup>7</sup> D.W. Welsh<sup>7</sup> A.C. Marvin<sup>7</sup>

<sup>1</sup>The Institute of the Basics of Electrical Engineering and Measurement Science, Leibniz University of Hannover, Appelstraße 9A, Hannover 30167, Germany

<sup>2</sup>The Universitat Politècnica de Catalunya, Campus Nord C4 Jordi Girona 1-3, Barcelona 08034, Spain

<sup>3</sup>Department of Electrical Engineering and Computer Science, University of Liège, Insitut Montefiore B28, Liège 4000, Belgium

<sup>4</sup>Katholieke Hogeschool Brugge-Oostende, Zeedijk 101, Oostende B-8400, Belgium

<sup>5</sup>The Open University, The Open University in the North West, 351 Altincham Road, Sharston, Manchester M22 4 UN, UK

<sup>6</sup>The Institute d'Electronique, de Microélectronique et de Nanotechnologies (IEMN), University of Lille, Bat. P3, Villeneuve d'Ascq Cedex 59655, France

<sup>7</sup>Department of Electronics, University of York, Heslington York, YO10 5DD, UK  
E-mail: battermann@geml.uni-hannover.de

**Abstract:** Different approaches for the characterisation of relevant parameters of the low-voltage mains network, used for high-speed data transmission (BPL, broadband over power line) are described. Part 1 of the paper depicts the disturbance scenario of these BPL devices and the motivation will be given for the development of a new measurement procedure in CISPR for the estimation of the high-frequency characteristics of AC mains network. The improvements of the measurement method is not restricted to BPL applications, but can also be applied to other wire-based telecommunication systems. Part 2 of the paper shows the definitions and comparisons of different symmetry factors. The transfer of the results on the compliance test for BPL devices will be shown.

## 1 Introduction

The standardisation process to assess RF disturbances originating from broadband over power line (BPL), power-line communication (PLC) or power-line telecommunication equipment is still on going. Many home-plug BPL modems are in use for in-house communication as a substitute for Ethernet or video wiring. The customer must make a choice between DSL routers with an integrated wireless local area network (WLAN) or an in-house BPL modem.

Because of the high market penetration with DSL access, this will increase the number of installed BPL devices and could possibly result in a higher number of cases of potential harmful interference between the BPL modem as a noise source and a short-wave radio receiver as the victim [1–4].

One of the main tasks for standardisation is to define the limits and appropriate compliance test methods with measurement setups. Since communication of BPL devices is conducted via the AC mains port, the limits

found in CISPR 22 [5] for the AC mains port should apply. Under worst-case conditions, these limits can, however, be denoted as an asymmetrical or common-mode RF disturbance voltage. In order to prevent an overestimation of the disturbing effects of the wanted differential-mode signal, it is proposed to use a telecommunication impedance stabilisation network (T-ISN) for the compliance test of BPL devices in the conducted disturbance measurement [5]. For this T-ISN, the high-frequency (HF) characteristics have to be defined. It has to provide an HF symmetry at its mains port that is representative of the average HF symmetry of the typical low-voltage AC mains network.

This paper presents the measurement methods to determine the symmetry factors that can be used to develop a T-ISN. For a systematic study, it is necessary to analyse the disturbance at each node, from transmitter to receiver, including the channel transfer function between the source of interference and the victim.

### 1.1 Mains decoupling factor: disturbance scenario of electronic devices

CISPR 16-4-4 [6] states that conducted coupling between the disturbance source and the victim dominates in the frequency range below 30 MHz. But CISPR does not describe a method to estimate this coupling, although the values may be useful for the characterisation of the disturbance potential of BPL devices. Therefore the standardisation committees in CISPR started a discussion of the mains decoupling factor that has been defined in the CISPR Report 31 in 1967. The basic idea was to detect the decoupling between a disturbance source and the resulting voltage at the antenna connected to a receiver. The resulting RF disturbance voltage level should be measured across the antenna termination impedance, that is, across the RF input impedance of the first RF amplifier stage of the receiver. This was, however, not the case when the measurements were made in the late 1960s of the last century. At that time, the antenna terminal voltage was measured with a battery-operated measuring receiver in conjunction with a high-impedance probe. The reason for the disturbance is the unwanted emission from the device. With this approach, it is possible to define the permissible level of a disturbance voltage at the source based on the highest acceptable level of the disturbance voltage appearing at the receiver that still safeguards a sufficient signal-to-noise ratio (SNR). The schematic measurement setup used in the measuring campaign in the 1960s is shown in Fig. 1.

The signal is injected into the phase ( $L$ ) and neutral ( $N$ ) conductor in parallel with the protective earth (PE) conductor acting as counterpoise. Therefore it is

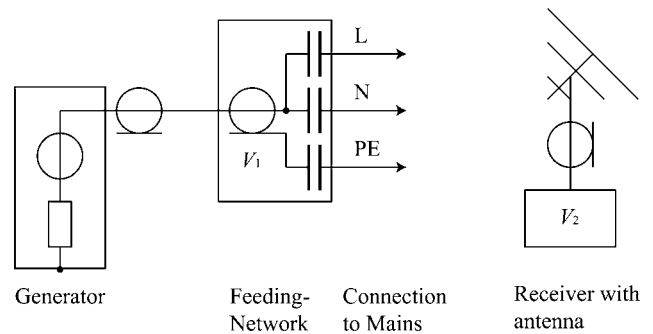


**Figure 1** Schematic setup for the measurement of the mains decoupling factor

a common-mode feeding with respect to phase and neutral conductors. The receiver with the antenna is isolated without a connection to mains. The voltage  $V_2$  is the meter reading of the receiver.  $V_1$  has to be measured with an artificial mains network at a conducted electromagnetic interference test setup that conforms to CISPR 22 [5]. The mains decoupling factor  $D_M$  is the logarithmic ratio of both voltages as shown in (1)

$$D_M = 20 \cdot \log \left( \frac{V_1}{V_2} \right) \quad (1)$$

### 1.2 Description of the disturbance scenario of BPL devices

Today, a typical home-plug power-line modem has a highly symmetrical structure and the feeding could be represented by a pure differential-mode signal between the phase ( $L$ ) and neutral ( $N$ ) conductor. Contrary to the unwanted emission of other types of electric or electronic apparatus, which eventually was the motivation for the measurement technique of the mains decoupling factor, the differential-mode excitation of BPL devices is a wanted signal used for data transmission. Furthermore, the PE is not connected to the modem because the modem is completely isolated (protection class II). Nevertheless, the USB or Ethernet connection between the PC and the modem acts as a counterpoise. The modem can cause a common-mode current by itself (launched common mode, LCM) and a common mode due to mode conversion caused by the low symmetry of the AC mains network (converted common mode, CCM). The illustrated measurement setup of the mains decoupling factor in Fig. 1 does not reproduce the depicted typical disturbance scenario with a modern in-house BPL modem. In order to align the measurement setup described in CISPR Report 31 (Fig. 1) with the conditions found in practice, some changes have been made, which are depicted in Fig. 2. The modified setup reproduces the disturbance scenario in a more realistic way.

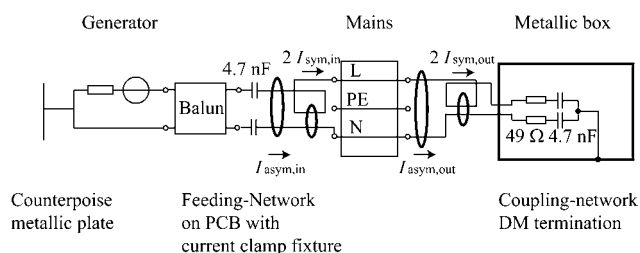


**Figure 2** Schematic illustration of the measurement setup for an estimation of the HF characteristics of the mains network

A comb generator feeds a symmetrical (alternatively an asymmetrical signal) between phase ( $L$ ) and neutral conductor ( $N$ ) that is terminated at the load position with about  $100 \Omega$  – the typical differential-mode characteristic impedance of mains cabling. A metallic box or radio which acts as the common-mode load is connected to the mains with a coupling network that contains a high-pass filter. Fig. 7 shows a radio dummy instead of the metallic box. Both setups represent the same common-mode impedance to the mains. This is the typical situation for a mains-powered receiver with a mains cable or a power supply without common-mode chokes on the mains wire. The currents at the input and output of the mains network are measured. The return path for the asymmetrical current is the surrounding earth (capacitive coupling). Different measurement actions revealed [7, 8] that the interfering effect to a receiver with a rod antenna is stronger when the receiver is mains powered, when compared with battery powering. The reason for this is the common-mode current flowing from the mains over the chassis to the surrounding earth. This will be explained in detail in Section 2.3.

## 2 Measured quantities and measurement setup

### 2.1 Reasons for the measurement of currents

In the past, all symmetry values of telecom cables were based on voltages (e.g. longitudinal conversion loss [9]). The original mains decoupling factor also was based on voltages. The measurement of the voltages  $V_1$  and  $V_2$  (Fig. 1) could be done in a simple way because  $V_1$  can be measured against the potential of PE and  $V_2$  is the meter reading of the receiver. With respect to the new feeding method between the phase and neutral (Fig. 2), it is necessary to measure the differential-mode voltage and the common-mode voltage at the feed point and at the load (receiver). But the common-mode voltage has to be measured against the surrounding earth potential, which is a non-existing pole and cannot be connected. A possible way is the use of a capacitive voltage clamp but the necessary

metallic counterpoise also influences the measured common-mode voltage.

For these reasons, the common-mode current is measured with a current clamp instead of the measurement of voltage. Furthermore, it is well known that the disturbance quantity is the common-mode current on the mains, which is also called antenna mode current [8, 10].

### 2.2 Feeding circuit for the mains

For the purpose of this research work, a battery-powered comb generator is used as signal generator with a metallic plate of  $0.5 \text{ m}^2$  as a defined counterpoise (Fig. 3a). This is only one possible type of generator that can be used for these measurements. The output is connected to a printed circuit board (PCB). The balun and the coupling capacitors are already included on the PCB. The output is connected to a mains socket. Furthermore, the PCB includes a dedicated fixture for the current clamp (Fig. 3b). Former measurements show that the current probe for the measurement of the feeding currents influences the results when it has been changed between differential- and common-mode current measurements. The reason for this is the changing parasitic capacitance of the probe, which results in a leaking common-mode current. The Technical University of Catalonia (UPC) developed a PCB that enables a well-defined fixture of the current probe to reduce the influences. The change from differential- to common-mode measurement is simply performed by jumpers. This new measurement setup further improved the reproducibility. To keep the impedances at the input constant, the counterpoise is used for both, common- and differential-mode feedings. For the common-mode coupling path, the distance between the metallic plate and ground has to be kept constant to obtain comparable results.

### 2.3 Coupling to the load

A metallic box is used as a common-mode load or to simulate a mains-powered device. The dimensions of

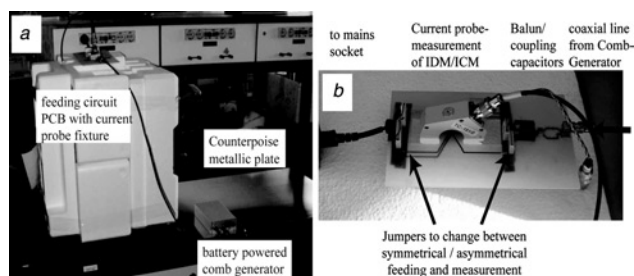


**Figure 3** Feeding circuit of the mains

a Feeding circuit with comb generator and counterpoise  
b PCB for the feeding with balun, coupling capacitors and a fixed probe position for the current clamp

the box are 300 mm × 200 mm × 100 mm. A second PCB for the measurement of the differential- and common-mode currents to the box is located directly at the connection to the mains socket (Fig. 4).

The common-mode impedance of the coaxial line from the current clamp to the measurement equipment is increased by a common-mode choke (Fig. 7). It contains a series of ferrite cores optimised for different frequency ranges and low capacitive coupling between input and output. It provides a broadband common-mode attenuation of at least 20 dB measured in a 100 Ω jig. This choke is important because the common-mode impedance of the equipment used for the current measurement could be lower than the common-mode impedance of the metallic box. This would result in a common-mode leakage current. The effect is depicted in Fig. 5.

From the impedance point of view, the measurement equipment connected to the current clamp would change the common-mode impedance that could be seen from the socket. But for repeatable measurements, the impedances have to be constant and they may be influenced only by different capacitive couplings of the metallic box to the surrounding environment ( $I_{\text{asym,Chassis}}$ ,  $I_{\text{asym,Ant}}$  in Figs. 4 and 6). This phenomenon of capacitive coupling will occur for all equipments and devices connected to a power cord to the mains. Especially, it will have the same effect on a receiver and it changes the  $I_{\text{asym,out}}$  to the chassis of the receiver, which will cause malfunctioning of the receiver.

## 2.4 Equivalence between $I_{\text{asym,out}}$ and the voltage induced at the antenna of a receiver

First, a radio dummy has been used, which consists of a metallic box with rod antenna (Fig. 6) to comply with the CISPR disturbance model. The complete setup at the load position is depicted in Fig. 7b. The PCB for

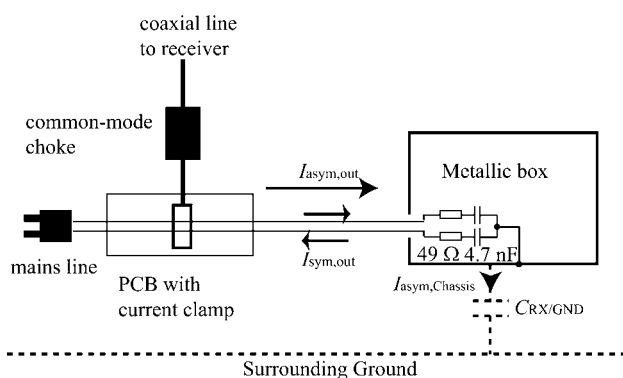


Figure 4 Schematic of the measurement setup at the load

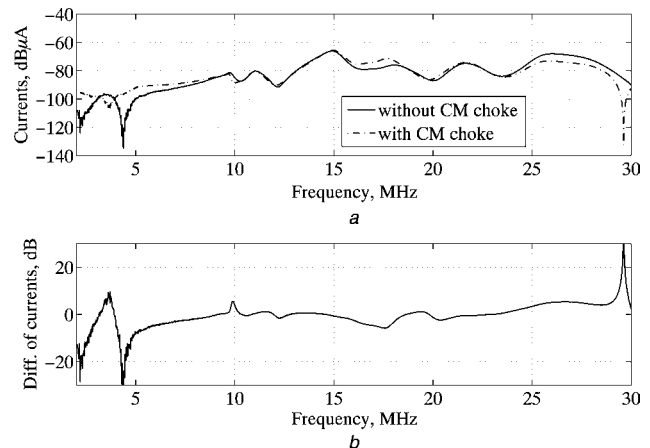


Figure 5 Use of a common-mode choke on the coaxial line to the current clamp

a Measurements with/without the common-mode choke

b Difference of the measured common-mode current due to the use of a common-mode choke on the coaxial line to the current clamp

the current measurement is directly connected to the socket and to the metallic box/receiver (wooden box). The metallic box is on the lower right side of the picture and it is covered by wood due to safety reasons. The common-mode impedance of the coaxial cable from the current clamp to the measurement receiver is increased with a common-mode choke that is depicted in detail in Fig. 7a. The rod antenna on top of the metallic box is connected to a battery-powered CISPR 25 impedance converter that is also

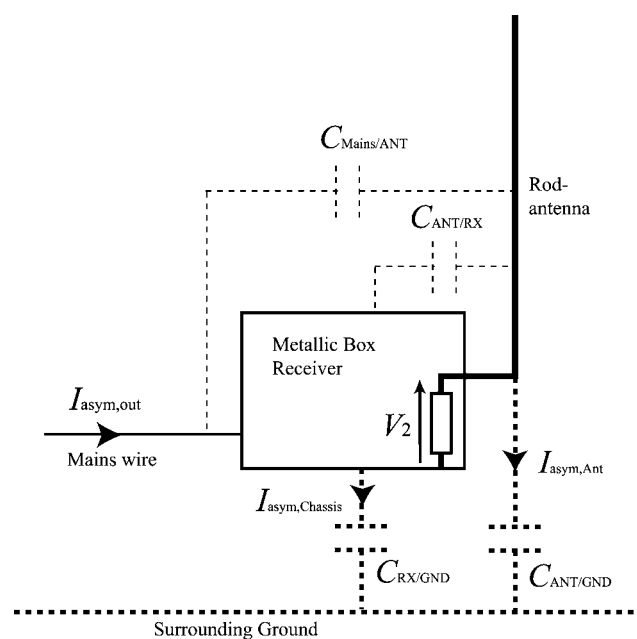
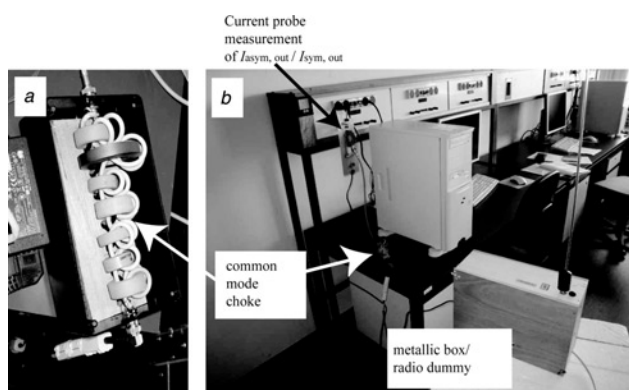


Figure 6 Schematic of the setup at the load with corresponding current divider



**Figure 7** Common-mode impedance of the coaxial line from the current clamp to the measurement equipment is increased by a common-mode choke

- a Common-mode choke  
b Measurement setup at the load

included in the box. It transforms the high impedance feed point of the rod antenna in the range of 100 k $\Omega$  to 50  $\Omega$ . The output of the impedance converter is connected to a fibre-optic link to avoid any galvanic connection between the radio dummy and the measurement receiver. By this way, it is possible to measure the voltage at the termination resistor of the rod antenna without any galvanic connection to external measurement equipment.

In order to reduce the complexity of the measurement setup with radio receiver and fibre-optic connection, the question if there is any parameter proportional to the interfering signal at the antenna input of a receiver is raised. For this analysis, Fig. 8 shows the antenna voltage and the current to the chassis of the receiver. The calculated transfer

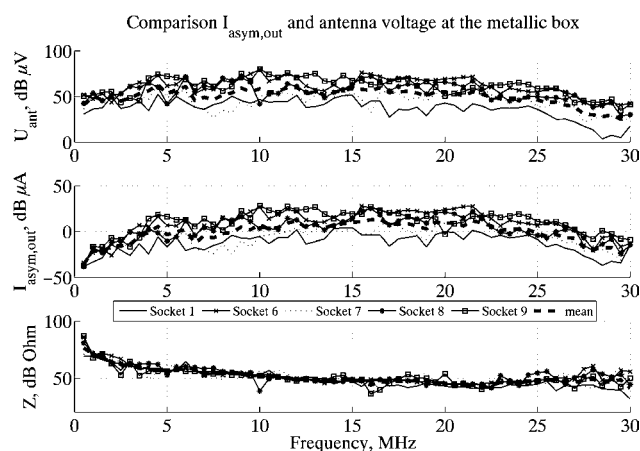


**Figure 8** Comparison of the antenna feed-point voltage at the metallic box (upper diagram) and the common-mode current (diagram in the middle) – the lower diagram shows the resulting transfer impedance  $Z$

impedance  $Z$  (in the bottom diagram) is depicted as

$$Z = 20 \cdot \log \left( \frac{V_2}{I_{\text{asym,out}}} \right) \quad (2)$$

The transfer impedance shows the capacitive behaviour of the rod antenna and any amplification of the impedance converter in the metallic box. It may be concluded that there is a very good proportional agreement between the measured  $I_{\text{asym,out}}$  and the voltage over the antenna input impedance  $V_2$  of a receiver [7]. The common-mode current  $I_{\text{asym,out}}$  flowing into the metallic box is the dominant reason for the feed-point voltage  $V_2$  at the rod antenna (Fig. 6). The common-mode current  $I_{\text{asym,out}}$  from the mains connection is split due to capacitive coupling mainly into the current from the metallic box to ground ( $I_{\text{asym,Chassis}}$ ) and the current  $I_{\text{asym,Ant}}$  from the rod antenna to ground. Therefore there is no need to use a radio dummy for further measurements. By measuring the  $I_{\text{asym,out}}$ , the amount of interference is obtained, if the common-mode load conditions are accounted. This can be done by using a metallic box or plate and an appropriate RC circuit, as shown in Fig. 4.

### 3 Measurements under real conditions

The measurements have been performed in different houses and installations. The results that are presented in this paper are obtained from measurements in the Leibniz University of Hannover. The floor plan is shown in Fig. 9. Different power systems exist in parallel. Two big lines start from the power distribution room in the centre of the floor and move along the corridors to the laboratories. The examined sockets are depicted by numbered circles. Sockets 2 and 5 are fed from a different power system and even a different transformer (10 kV/400 V) with a resulting wire length of approximately more than 200 m to the feed point. Therefore the attenuation between the fed socket and the load socket is too high to provide a reasonable SNR. This is the same for socket 4 that is connected to a PC room in parallel with 20 PCs that reduces the differential-mode signal significantly. These sockets have been removed for further analysis because they are not representative of in-house BPL modems or even for large buildings. The other sockets use the same transformer (10 kV/400 V) but on different lines that move along the corridors. Because of safety reasons, all sockets in the laboratories are connected to the supply line with a relay box or a switch. The layout is a star topology without any inductive over-current protection or earth leakage trip. The wire length between the source and

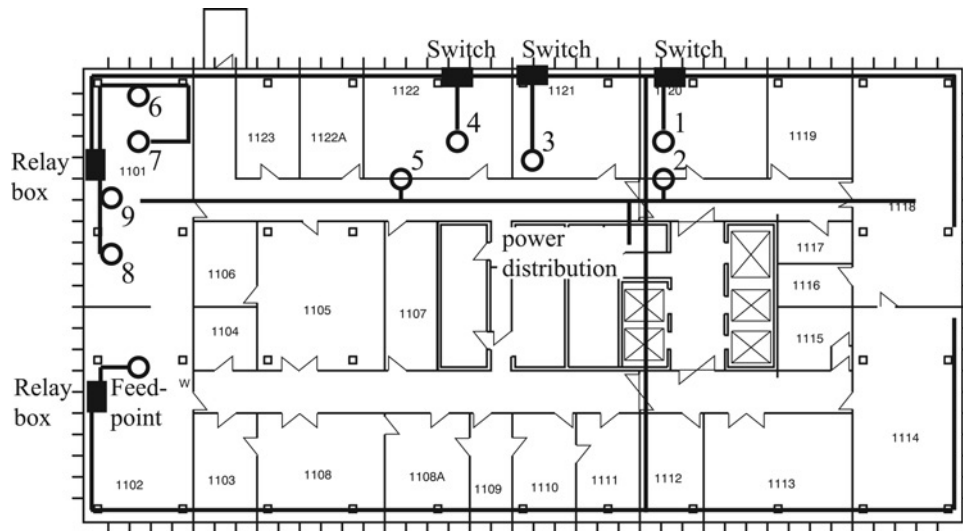


Figure 9 Floor plan of the institute (scaling of the tick-marks on the boundary is 1 m)

load is quite high and up to about 80 m for sockets 6–9. The feeding of the high-frequency signal is done in room 1102. Table 1 summarises the location of the sockets and the used phases.

#### 4 Symmetrical and asymmetrical mains attenuation

When a signal is applied at one mains socket (Fig. 10, position A), differential- and common-mode signals that can be measured at the other sockets appear (Fig. 10, position B). The common-mode signal at socket B ( $G_{\text{asym,out}}$ ) is the disturbance quantity [8, 11]. Because of the mode conversion of the mains network, even feeding a highly symmetrical signal will produce an asymmetrical signal ( $G_{\text{asym,out}}$ ) at the

output. For this reason, two different coupling paths could be defined: (i) when a symmetrical signal ( $G_{\text{sym,in}}$ ) is applied at socket A and (ii) when an asymmetrical signal is applied ( $G_{\text{asym,in}}$ ).

The attenuation of a symmetrical (or differential mode) signal between the feeding (at position A) and the load socket (at position B) is  $A_{\text{sym}}$  (in dB)

$$A_{\text{sym}} \left| \begin{matrix} P1 \\ A \leftrightarrow B \end{matrix} \right. = G_{\text{sym,in}} \left| \begin{matrix} P1 \\ A \end{matrix} \right. - G_{\text{sym,out}} \left| \begin{matrix} P1 \\ B \end{matrix} \right. \quad (3)$$

The attenuation of an asymmetrical (or common mode) signal  $A_{\text{asym}}$  (in dB) between the feeding (at position A) and the load socket (at position B) is calculated as shown in (4)

$$A_{\text{asym}} \left| \begin{matrix} P2 \\ A \leftrightarrow B \end{matrix} \right. = G_{\text{asym,in}} \left| \begin{matrix} P2 \\ A \end{matrix} \right. - G_{\text{asym,out}} \left| \begin{matrix} P2 \\ B \end{matrix} \right. \quad (4)$$

Table 1 List of the different sockets with the place of installation, used power system and phases

Socket	Room	System	Phase system I
feeding	1102	I	L2
1	1120	I	L1
2	floor	II	other system
3	1121	I	L3
4	1122	I	L3
5	floor	II	other system
6	1101	I	L1
7	1101	I	L1
8	1101	I	L1
9	1101	I	L2

For practical measurements, it is essential to have well-defined differential- and common-mode impedances for all measurements. The impedance conditions of the feeding and the load unit have to be kept constant for all measurements.

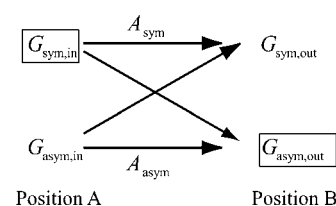
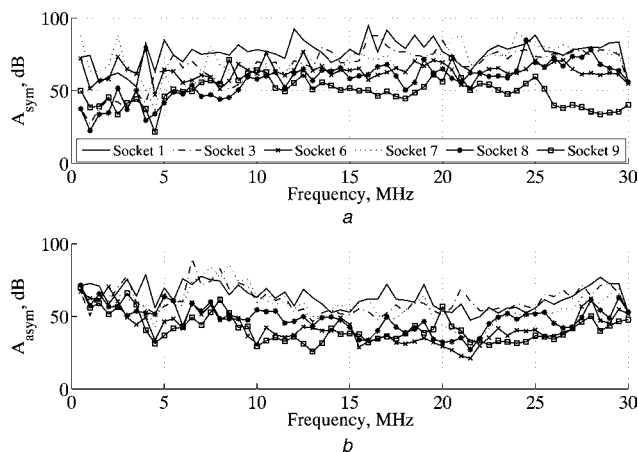


Figure 10 Schematic matrix of the measured signals and the attenuations



**Figure 11** Attenuation of signals

a Symmetrical  
b Asymmetrical

In this paper, current has been used for the quantity  $G$ , although it is also possible to use the voltage, power or field strength, if the quantity is representative of the disturbance. The symmetrical attenuation is shown in Fig. 11a. In the low-frequency range, two groups exist: sockets 6, 8 and 9 and sockets 1, 3 and 7. This correlates with the installation. Sockets 1, 3 and 7 are connected in parallel with devices with low differential-mode impedance (e.g. line filters of PC), which results in a high attenuation. The attenuation of the asymmetrical signal is depicted in Fig. 11b and it is generally lower than the attenuation of the symmetrical signal. Again two different clusters of sockets exist.

The mains symmetry factor is defined as the difference between a fed differential-mode signal ( $G_{\text{sym,in}}$ ) and a separately fed common-mode signal ( $G_{\text{asym,in}}$ ) that produce the same common-mode output at position B ( $G_{\text{asym,out}}$ ). It will be discussed in more detail in the second part of this paper. The determined symmetrical and asymmetrical attenuations will be used for the calculation of the mains symmetry factor.

## 5 Conclusion

This paper presented a new measurement method to describe the attenuation of the mains network. The specific characteristics of the measurement setup to measure the symmetrical and asymmetrical attenuations have been explained in detail. In the second part of this, detailed analysis of the measured data to obtain the mains symmetry factor  $M_{S, F}$  will be presented. This factor is necessary to characterise the HF symmetry of the mains network and to build appropriate T-ISO for electromagnetic compatibility (EMC) compliance tests of BPL or telecommunication devices.

## 6 Acknowledgments

Major parts of this work are based on the results obtained from [11]. The measurements and further improvements of the measurement setup emerged from the European Cooperation in the field of Scientific and Technical Research COST 286 with the topic 'EMC in diffused communications systems'. The Joint Technical Action 2 (JTA2) deals with the 'EMC analysis of LF unstructured telecom networks'. Further details can be found in [12]. We are glad to acknowledge the help and assistance of the European Action COST 286 Team throughout the investigations under this Joint Technical Action. This work was done with support and on behalf of the European Action COST 286 (electromagnetic compatibility in diffused communications systems).

## 7 References

- [1] STECHER M: 'EMC aspects of powerline communication'. EMC Europe, Int. Symp. EMC, Brugge, Belgium, September 2000
- [2] WELSH DW: 'Investigation of likely increase in established radio noise floor due to widespread deployment of PLT, ADSL and VDSL broadband access technologies'. EMC Zurich Symp., March 2001
- [3] HANSEN D: 'Megabits per second on 50 Hz power lines'. Proc. 15th Int. Wroclaw Symp. EMC, Wroclaw, Poland, June 2000, pp. 107–110
- [4] HANSEN D: 'Megabits per second on powerlines', *IEEE EMC NewsL.*, 2001 Winter), pp. 17–21
- [5] CISPR 22 Ed. 5.2 b: 'Information technology equipment – radio disturbance characteristics – limits and methods of measurement', 2006
- [6] CISPR/TR 16-4-4 Ed. 1.0: 'Specification for radio disturbance and immunity measuring apparatus and methods – part 4-4: uncertainties, statistics and limit modelling – statistics of complaints and a model for the calculation of limits', 2003
- [7] BATTERMANN S, GARBE H, DUNKER L: 'Measurement method to describe the attenuation characteristics of the mains network'. EMC Europe'. Int. Symp. EMC, Barcelona, Spain, September 2006, pp. 414–419
- [8] BATTERMANN S, GARBE H: 'Interference potential of PLC and measurement of mains characteristics'. Proc. 18th Int. Wroclaw Symp. EMC, Wroclaw, Poland, June 2006
- [9] MACFARLANE IP: 'A probe for the measurement of electrical unbalance of networks and devices', *IEEE Trans. EMC*, 1999, **41**, (1), pp. 3–14

[10] PAUL CR: 'Introduction to electromagnetic compatibility' (Wiley, New York, 1992)

[11] <http://www.bundesnetzagentur.de/media/archive/6578.zip>, accessed June 2007

[12] Special workshop on BPL (organized by COST 286), EMC Europe, 04–08 September 2006, Barcelona, Spain, available at: <http://www.emc.york.ac.uk/cost286/>, accessed June 2007